Development 137, 2507-2517 (2010) doi:10.1242/dev.049700

hand2 and Dlx genes specify dorsal, intermediate and ventral domains within zebrafish pharyngeal arches

Jared Coffin Talbot[1,*], Stephen L. Johnson[2] and Charles B. Kimmel[1]

SUMMARY

The ventrally expressed secreted polypeptide endothelin1 (Edn1) patterns the skeleton derived from the first two pharyngeal arches into dorsal, intermediate and ventral domains. Edn1 activates expression of many genes, including *hand2* and Dlx genes. We wanted to know how *hand2*/Dlx genes might generate distinct domain identities. Here, we show that differential expression of *hand2* and Dlx genes delineates domain boundaries before and during cartilage morphogenesis. Knockdown of the broadly expressed genes *dlx1a* and *dlx2a* results in both dorsal and intermediate defects, whereas knockdown of three intermediate-domain restricted genes *dlx3b*, *dlx4b* and *dlx5a* results in intermediate-domain-specific defects. The ventrally expressed gene *hand2* patterns ventral identity, in part by repressing *dlx3b/4b/5a*. The jaw joint is an intermediate-domain structure that expresses *nkx3.2* and a more general joint marker, *trps1*. The jaw joint expression of *trps1* and *nkx3.2* requires *dlx3b/4b/5a* function, and expands in *hand2* mutants. Both *hand2* and *dlx3b/4b/5a* repress dorsal patterning markers. Collectively, our work indicates that the expression and function of *hand2* and Dlx genes specify major patterning domains along the dorsoventral axis of zebrafish pharyngeal arches.

KEY WORDS: Dlx, Hand2, Joint, Patterning, Skeleton, Zebrafish

INTRODUCTION

Specification of pharyngeal arch-derived facial skeleton by transcription factor-encoding genes is a topic of considerable recent interest. Pharyngeal arches are comprised of neural crest-derived mesenchymal cells, with mesoderm-derived cores, surrounded medially by endoderm and laterally by ectoderm. Edn1 is a secreted protein important for dorsoventral jaw patterning: in mouse, mutations in *Edn1* and its receptor *Ednra* cause homeotic transformations of lower jaw skeleton into upper jaw skeleton (Ozeki et al., 2004; Ruest et al., 2004). Studies of Edn1 signaling in zebrafish (*Danio rerio*) indicate that early pharyngeal arch patterning results in discrete dorsal, intermediate and ventral domains (D-I-V) in pharyngeal arch mesenchyme and pharyngeal-arch-derived skeleton (Kimmel et al., 1998; Miller and Kimmel, 2001; Miller et al., 2000; Miller et al., 2003; Walker et al., 2006). Edn1 is known to activate expression of many genes proposed to mediate D-I-V patterning, including *hand2*, *gsc*, *nkx3.2* (formerly *bapx1*) and the Dlx genes (Miller et al., 2000; Miller et al., 2007; Walker et al., 2006). However, the boundaries of early D-I-V patterning genes have not yet been examined at later timepoints when the D-I-V skeletal regions are visible. In this study, we propose a unified definition of D-I-V domains, and examine interactions between genes that pattern these domains. We place a particular focus on the patterning of intermediate-domain joints and jointed skeleton. In this study, 'joint' refers specifically to mesenchyme connecting early larval skeletal elements, whereas 'joint region' includes both this joint mesenchyme and connected skeleton. We refer to the joint between Meckel's and palatoquadrate cartilages as the 'jaw joint' of larval zebrafish.

Dlx genes are homeodomain-containing transcription factors, homologs of the single *Distal-less* gene in *Drosophila* (for a review, see Panganiban and Rubenstein, 2002). Mammalian Dlx genes are found in three bi-gene clusters (Qiu et al., 1997). Zebrafish also have three Dlx bi-gene clusters, containing *dlx1a* and *dlx2a*, *dlx3b* and *dlx4b*, *dlx5a* and *dlx6a,* as well as two additional Dlx genes, *dlx2b* and *dlx4a* (Stock et al., 1996). The two genes in each Dlx bi-gene cluster are approximately co-expressed (Ellies et al., 1997; Qiu et al., 1997), probably owing to shared enhancers (Ghanem et al., 2003; Park et al., 2004; Sumiyama et al., 2003). In mouse and zebrafish, functional redundancy is present both within and between these bi-gene pairs (Depew et al., 2005; Jeong et al., 2008; Qiu et al., 1997; Sperber et al., 2008; Walker et al., 2006). Within mouse pharyngeal arches, *Dlx1* and *Dlx2* (collectively referred to as *Dlx1/2*) expression extends further dorsally than *Dlx5/6*, which themselves show expression further dorsal than *Dlx3/4* (Depew et al., 2002; Qiu et al., 1997). *Dlx1*$^{-}$*;Dlx2*$^{-}$ mice primarily show dorsal skeletal defects (Qiu et al., 1997), and loss of dorsal specific molecular markers (Jeong et al., 2008). Conversely, *Dlx5*$^{-}$*;Dlx6*$^{-}$ mice show homeotic transformations of lower jaw into upper jaw, corresponding to the exclusion of *Dlx5/6* expression from dorsal arch regions (Beverdam et al., 2002; Depew et al., 2002). The skeletal homeosis of *Dlx5*/6 loss is mirrored by a ventral expansion of dorsal molecular markers, whereas several ventral markers (including *Hand2*) are lost.

Hand2 encodes a basic helix-loop-helix protein crucial for ventral facial pattern. Mice carrying a deletion in the pharyngeal arch-specific promoter of *Hand2* have dramatically shortened lower jaws, but relatively normal patterning in joint regions and the upper jaw (Yanagisawa et al., 2003). When *Hand2* is ectopically expressed throughout pharyngeal arches the upper jaw was partially transformed into an ectopic lower jaw (Sato et al., 2008). Thus, in mouse, the Edn1 targets *hand2* and Dlx are directly implicated as homeotic selector genes along the pharyngeal arch dorsoventral axis.

[1]Institute of Neuroscience, University of Oregon, Eugene, OR 97403, USA.
[2]Washington University in St Louis, St Louis, MO 63110, USA.

*Author for correspondence (jtalbot@uoregon.edu)

Accepted 18 May 2010

In zebrafish, *dlx3b* and *dlx5a* are redundantly required for patterning specifically within intermediate domain-derived skeleton (Walker et al., 2006). By contrast, zebrafish *hand2* nulls exhibit loss of lower jaws, but not upper jaws (Miller et al., 2003). *hand2* is expressed ventral to *nkx3.2*, a marker of the jaw joint region (Miller et al., 2003). In zebrafish, *hand2* mutants, *nkx3.2* expands ventrally, indicating that *hand2* patterns lower jaw identity in part by repressing jaw joint identity (Miller et al., 2003). However, it was unclear whether *hand2* represses intermediate domain identity, because *hand2* mutants consistently lose jointed-jaw skeleton (Miller et al., 2003).

Fate-mapping experiments have indicated approximately where skeletal patterning domains arise within early pharyngeal arches (Crump et al., 2006; Crump et al., 2004; Eberhart et al., 2006). However, these fate maps lacked the precision to directly connect early gene expression patterns to later skeletal shapes. Here, we present expression patterns that allow us to precisely define the dorsal, intermediate and ventral domains within zebrafish pharyngeal arches. We propose that the ventral domain comprises the *hand2*-expressing pharyngeal arch region, and the skeletal elements that are formed in this region. The ventral domain contains most of Meckel's and ceratohyal cartilages, and the dentary bone. The intermediate domain is the region of pharyngeal arches that expresses all Dlx genes, besides *dlx2b* (which is not expressed in anterior arches). Expression of the most restricted Dlx gene, *dlx4a*, reveals the borders of the intermediate domain. The intermediate domain includes the jaw joint region, and the second arch joint region, as well as the opercle and branchiostegal bones. Arch mesenchymal expression of *dlx3b* and *dlx4b* is also restricted to the intermediate domain. The dorsal domain is the region of the pharyngeal arch dorsal to *dlx4a* expression. Because *dlx2a* is expressed throughout the arch dorsoventral axis, co-labeling of *dlx2a* and *dlx4a* reveals the dorsal domain. The dorsal domain contains most of the palatoquadrate cartilage, including the distinctive pterygoid process, the hyomandibular cartilage and the maxillary bone. *dlx5a* and *dlx6a* expression does not correspond to a single domain.

In addition to defining D-I-V domains, this report examines the functional requirements for D-I-V patterning. We show that along with *dlx3b* and *dlx5a*, *dlx4b* is also redundantly required for intermediate domain skeleton. We report a transgenic revealing the expression pattern of *trps1*, a general marker of skeletal joint identity. We show that *nkx3.2* and *trps1* require *dlx3b/4b/5a* function for normal expression. We examine regulation between domains, noting that *hand2* inhibits ventral expression of *dlx3b*, *dlx4a*, *dlx4b* and *dlx5a*. In *hand2* mutants, *nkx3.2* and *trps1* expand to fill ventral space beneath expanded intermediate domain skeleton. However, even in *hand2* mutants, expression of *trps1* and *nkx3.2* still requires *dlx3b/4b/5a* function. Despite differences in patterning ventral versus intermediate domains, we provide evidence that *hand2* and *dlx3b/4b/5a* act in concert to repress dorsal domain identity.

MATERIALS AND METHODS

Fish maintenance, husbandry and strains

Fish were raised and maintained under standard conditions and staged as described previously (Kimmel et al., 1995; Westerfield, 1995). Mutant lines were maintained on the AB background, and morpholinos were injected into AB fish. *Df(Chr1)hand2*^{S6} (a null allele, hereafter: *hand2*^{S6}) and *Is(Chr1)hand2*^{C99} (a hypomorphic allele, hereafter: *hand2*^{C99}) homozygotes were identified using previously described fully penetrant phenotypes, including dramatic heart defects (Miller et al., 2003; Yelon et al., 2000). *edn1* mutants were identified as previously described (Miller et al., 2000).

trps1^{j1271aGt} (at most a hypomorphic allele) and *dlx5a*^{j1073Et} (a likely hypomorph, based on comparison with morpholinos) were generated using the *Tol2* transposon T2KSAG, which contains enhancerless *eGFP* (Kawakami et al., 2004), during a screen for vital markers with specific expression patterns. *trps1*^{j1271aGt} and *dlx5a*^{j1073aEt} stocks have been submitted to ZIRC. After identification, carriers were outcrossed to AB background fish for several generations. Tail-PCR (Parinov et al., 1999) was used to identify genomic flanking regions, revealing that the J1271a insertion is at chr19: 43671269, inside the first intron of *trps1*, and the J1073a insertion site is chr19: 40245837, inside the first exon of *dlx5a*. A PCR primer in the transposon sequence (GCAAGGGAAAATAG-AATGAAGTG) and primers in the flanking genomic DNA sequence (*trps1*^{J1271aGt}: TGTATTTTGACTCCTCAGTTCTGC, TACGCTCGAG-TGAAGTGTGG or for *dlx5a*^{J1073Et}: ATTCCTGAGACGGATGATGC, CGTAACAGCGCAATTTAGGA) were then designed and tested on 24 embryos segregating the expression pattern to show that we had correctly identified the insertion generating the expression pattern.

Tissue labeling

Alcian Blue and Alizarin Red staining was as described (Walker and Kimmel, 2007). For vital bone staining, fish were treated overnight with 0.000033% Alizarin Red in embryo medium, followed by de-staining in embryo medium. Fluorescent RNA in situ hybridization was carried out with a protocol modified from those described previously (Jowett and Yan, 1996; Welten et al., 2006). DNP-labeled probes were revealed with tyr-Cy5, dig-labeled probes were revealed using tyr-Cy3, fluorescein-labeled probes were revealed with tyr-fluorescein (available from Perkin-Elmer). Our full RNA in situ protocol is available online (http://wiki.zfin.org/display/prot/Triple+Fluorescent+In+Situ). Probes used are *dlx2a* (Akimenko et al., 1994), *dlx3b* (Akimenko et al., 1994), *dlx5a* (Walker et al., 2006), *dlx6a* (Walker et al., 2006), *gsc* (Schulte-Merker et al., 1994), *dlx4a* (Ellies et al., 1997), *dlx4b* (Ellies et al., 1997), *hand2* (Angelo et al., 2000), *nkx3.2* (Miller et al., 2003), *sox9a* (Yan et al., 2002) and *eng2* (Ekker et al., 1992).

Antibody labeling was essentially as described (Nusslein-Volhard, 2002). For RNA in situ experiments and antibody staining experiments, embryos were raised in 0.0015% PTU (1-phenyl 2-thiourea) to inhibit melanogenesis (Westerfield, 1995). Confocal imaging was performed on a Zeiss LSM5 Pascal microscope, followed by image processing with Volocity software. Colors are digitally enhanced to increase visibility.

Morpholino oligo injection

Morpholinos are injected at 2-3 nl into one- to two-cell stage embryos. Translation blocking morpholinos to *dlx1a* (Sperber et al., 2008), *dlx2a* (Sperber et al., 2008), *dlx3b* (Liu et al., 2003) and *dlx5a* (Walker et al., 2007), as well as a splice blocking morpholino to *dlx4b* (Kaji and Artinger, 2004) were purchased from Gene Tools using previously described sequences. *dlx1a*-MO and *dlx2a*-MO have previously been shown to be specific and effective through RNA rescue, and knockdown of transgenic *dlx1a-GFP* and *dlx2a-GFP* expression (Sperber et al., 2008). We confirm that *dlx3b*-MO strongly reduces Dlx3b immunolabeling (data not shown) (Liu et al., 2003). We also confirm that *dlx4b*-MO strongly disrupts *dlx4b* transcripts (Kaji and Artinger, 2004), without affecting any other Dlx gene (data not shown). Furthermore, in support of previous work (Liu et al., 2003), co-injection of *dlx3b*-MO with *dlx4b*-MO phenocopies otolith losses seen in a deletion that contains *dlx3b* and *dlx4b* (data not shown). In addition to the *dlx5a* translation blocking morpholino, we tested a splice blocking morpholino to *dlx5a* (*dlx5aE2I2*-MO: 5′-TATTCCAGGAAATTGTGCGAACCTG-3′). This morpholino had only nominal effects on splicing, and produced a different phenotypic suite from either the *dlx5a* translation blocking morpholino or the *dlx5a* mutant. As a result, *dlx5aE2I2*-MO was not used in any further analysis.

RESULTS

dlx3b, *dlx4b* and *dlx5a* redundantly pattern intermediate domain skeletal identity

Co-injection of *dlx3b*-MO and *dlx5a*-MO causes intermediate-domain-specific defects without affecting dorsal or ventral structures (supporting Walker et al., 2006). Because *dlx4b* is in the same bi-gene cluster as *dlx3b* (Ellies et al., 1997), we hypothesized

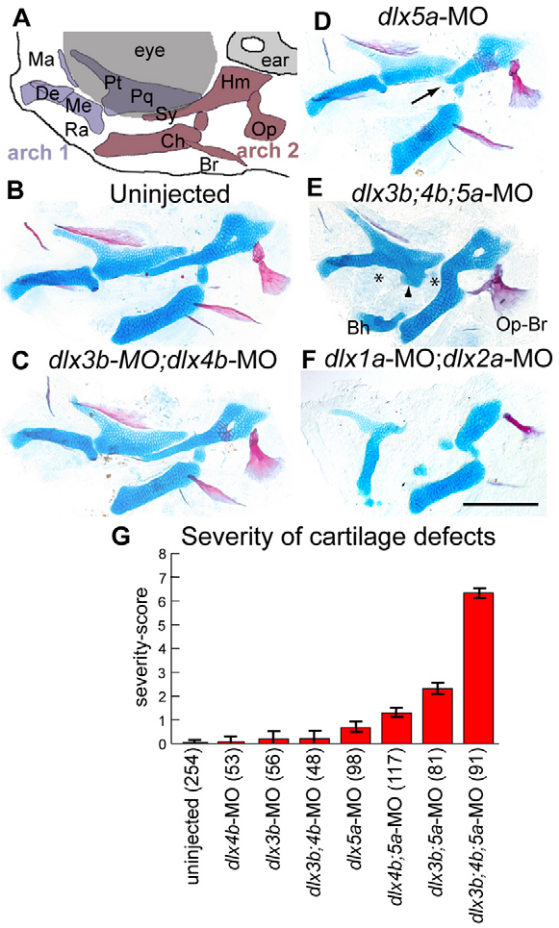

Fig. 1. *Dlx* function is required in intermediate domain skeleton. (**A**) Schematic of facial skeleton. Anterior is towards the left, dorsal is upwards. (**B-F**) Alcian Blue (cartilage) and Alizarin Red (bone) stained pharyngeal skeletons with *Dlx* morpholino treatments at 6 dpf. (B) Uninjected, (C) *dlx3b*-MO;*dlx4b*-MO and (D) *dlx5a*-MO fish look very similar, although *dlx5a*-MO sometimes causes shortened symplectic cartilages (arrow). (E) Injection of *dlx3b;4b;5a*-MO frequently causes dramatic skeletal defects, including joint loss (asterisks), fusion of OP and BSR bones (Op-Br), and ectopic processes attached to the palatoquadrate (arrowhead), or ventrally in the face. (F) By contrast, *dlx1a*-MO;*dlx2a*-MO injection causes defects in both dorsal and intermediate cartilages. (**G**) Plot of severity scores, showing that *dlx3b*-MO, *dlx4b*-MO and *dlx5a*-MO interact to create more than additive changes in intermediate domain skeletal phenotypes. Error bars are 95% confidence intervals, determined by ANOVA. Fish were scored bilaterally for prominent cartilage defects: first arch joint fusions, second arch joint fusions, symplectic defects, palatoquadrate defects and ectopic cartilages. Although each phenotype was seen at a range of expressivity, we assigned any defect a score of '1', irrespective of expressivity. The 'severity-score' is the sum of these defects for both sides of the fish. Skeletal elements indicated in A are the first arch-derived Meckel's cartilage (Me), including its retroarticular process (Ra), palatoquadrate (Pq) cartilage and its pterygoid process (Pt), as well as maxillary (Ma) and dentary (De) bones. The second arch gives rise to the ceratohyal cartilage (Ch), the hyosymplectic cartilage, which comprise distinctive hyomandibular (Hm) and symplectic (Sy) regions, as well as opercle (Op) and branchiostegal (Br) bones. A remnant of the basihyal cartilage (Bh) remains attached to the Ch in (E), as a mounting artifact. Scale bar: 100 μm.

that *dlx4b* also functions in intermediate domain patterning. Injection of *dlx4b*-MO and co-injection of *dlx3b*-MO with *dlx4b*-MO fails to cause striking phenotypes (Fig. 1C,G). However, co-injection of *dlx4b*-MO with *dlx5a*-MO causes low penetrance intermediate defects (Fig. 1G). Furthermore, fish co-injected with *dlx3b*-MO;*dlx4b*-MO;*dlx5a*-MO (henceforth called *dlx3b;4b;5a*-MO) show defects throughout the intermediate domain at high penetrance (Fig. 1E,G). This synergism indicates that *dlx3b*, *dlx4b* and *dlx5a* function partially redundantly in facial patterning. *dlx5a*^{J1271aEt} homozygotes co-injected with *dlx3b*-MO and *dlx4b*-MO fish showed defects specifically within the intermediate domain (data not shown), similar to *dlx3b;4b;5a*-MO fish. By contrast, the most frequent defect in uninjected *dlx5a*^{J1271aEt} homozygotes is a low penetrant shortened symplectic phenotype, similar to *dlx5a*-MO treatment (Fig. 1D and data not shown). Hence, with both a morpholino and a mutant, we confirm that *dlx5a* acts largely redundantly with *dlx3b* and *dlx4b* to pattern the intermediate domain.

dlx1a and *dlx2a* redundantly pattern intermediate and dorsal skeletal domains

In mouse, *Dlx1/2* have patterning requirements dorsal to *Dlx5/6* (Depew et al., 2002; Qiu et al., 1997). To test whether zebrafish *dlx1a*/*2a* has patterning requirements dorsal to *dlx3b/4b/5a*, we injected *dlx1a*-MO and *dlx2a*-MO together and separately. When injected alone, *dlx1a*-MO and *dlx2a*-MO cause little skeletal deformity (data not shown). In support of previous work (Sperber et al., 2008), *dlx1a*-MO;*dlx2a*-MO co-injection results in low penetrance intermediate domain defects (Fig. 1F). In addition, *dlx1a*-MO;*dlx2a*-MO-treated fish often showed defects within the dorsal domain cartilages (palatoquadrate and hyomandibular cartilage) (Fig. 1F), indicating that the dorsal requirements of *dlx1a* and *dlx2a* are conserved.

hand2 and *Dlx* delineate presumptive D-I-V domains

Several models have been proposed in which Dlx genes function combinatorially to impart dorsoventral skeletal identities (e.g. Depew et al., 2005; Walker et al., 2006). To understand *Dlx* combinatorial patterning properly, we must understand how the expression domains of the Dlx gene fit together, which we can directly assay using multi-color fluorescent RNA in situ hybridization.

dlx2a is expressed throughout the dorsoventral axis of pharyngeal arches, excluding mesodermal cores (Kimmel et al., 2001). At 36 hours post fertilization (hpf), *dlx4a* expression is intermediate along the dorsoventral axis of zebrafish pharyngeal arches, and expression is not seen in dorsal or ventral arch regions (Fig. 2F,K), as revealed by labeling *dlx4a* expression alongside *dlx2a*. *edn1* and *hand2* expression is ventral to *dlx4a* at 36 hpf (Fig. 2I,N). Thus, we can delineate the 36 hpf ventral domain by *hand2* expression, intermediate domain by *dlx4a* expression and dorsal domain by the expression of *dlx2a* dorsal to *dlx4a* (Fig. 2F). Similarly, at 36 hpf, *dlx3b* and *dlx4b* show intermediate specific expression, coincident with *dlx4a* boundaries within arch mesenchyme (Fig. 2C,H,M), although *dlx3b* also shows prominent epithelial expression (arrowheads in Fig. 2M).

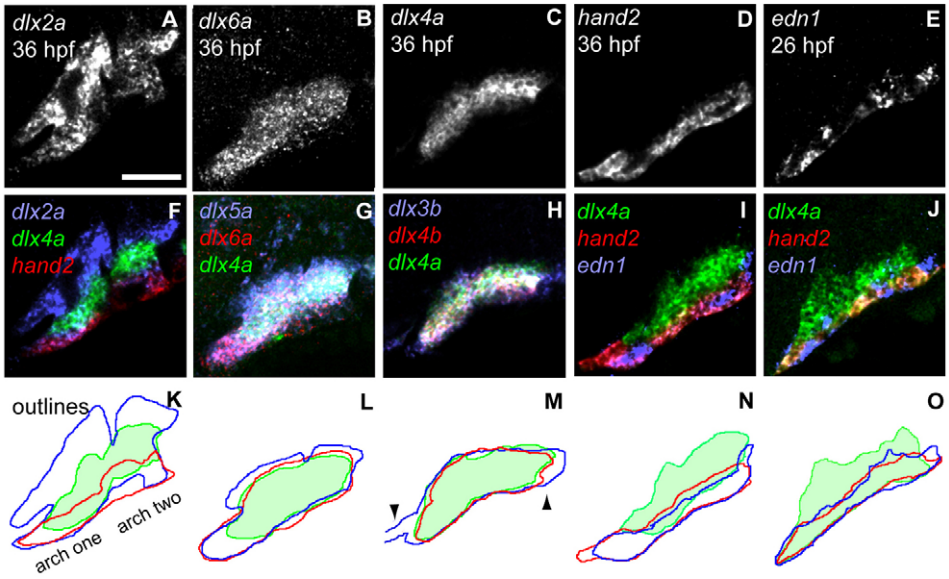

Fig. 2. Early patterning domains are revealed by Dlx gene, *hand2* and *edn1* expression. (**A-O**) Single confocal sections of fluorescent RNA in situ hybridization, anterior towards the left, dorsal upwards. The images in A-E are single channels from the confocal images in F-J. Outlines (K-O) of individual expression channels from F-J illustrate relative gene expression boundaries. (M) Arrowheads indicate *dlx3b* expression in the (left) stomodeum and (right) second endodermal pouch. Scale bar: 50 μm.

Other Dlx genes show broader expression than *dlx3b*, *dlx4b* and *dlx4a* at 36 hpf (Fig. 2). The dorsal limit of *dlx5a* expression lies between the dorsal limits of *dlx4a* and *dlx2a* expression (Fig. 2G). In arch 1, *dlx5a* expression extends ventral to *dlx4a* expression (Fig. 2G) and is co-expressed with *hand2* (data not shown), indicating that *dlx5a* is expressed in the first arch ventral domain. However, in the second arch, *dlx5a* expression shares a ventral boundary with *dlx4a* and is restricted from the ventral *hand2*-expressing region (Fig. 2G and data not shown). Matching the in situ analysis, Dlx3b protein is nested both dorsally and ventrally within the *dlx5a*^{j1073aEt}-expressing domain (see Fig. S1 in the supplementary material). *dlx5a* and *dlx6a* are largely co-expressed (Fig. 2B,G), although *dlx6a* has weaker expression intensity. Similar to *dlx2a*, the expression of *dlx1a* is seen broadly within pharyngeal arch mesenchyme, though with faint intensity (data not shown). *dlx2b* expression is not detected in the first two arches (Stock et al., 2006) (data not shown). Collectively, these results reveal a complex pattern of expression by 36 hpf, with the expression of *hand2* ventral to *dlx3b/4a/4b*, which is nested within *dlx5a/6a*, which themselves are nested within *dlx1a/2a* boundaries (Fig. 2K-O).

hand2 represses ventral expression of several *Dlx* genes

Although the expression of *dlx4a* is intermediate-specific at 36 hpf (Fig. 2I), the earliest *dlx4a* expression is found in both ventral and intermediate arches (Fig. 2J). This observation of ventral *dlx4a* loss between 26 hpf and 36 hpf in wild-type fish, combined with the previous observation that *hand2* represses *dlx3b* (Miller et al., 2003), suggested that *hand2* ventrally represses *Dlx* expression. Indeed, the expression of *dlx3b*, *dlx4b* and *dlx5a* expands ventrally in *hand2*^{S6} mutants at 36 hpf (Fig. 3). In wild-type fish, first arch expression of *dlx5a* extends more ventrally than *dlx3b* and *dlx4b*, whereas in *hand2*^{S6} mutant fish, the three genes share a ventral expression border (Fig. 3C,D). Antibody staining for Dlx3b also expands ventrally in *hand2*^{S6} (data not shown). Furthermore, in *hand2*^{S6} fish, the expression of *dlx4a* expands, and fills the mesenchyme around *edn1*-expressing ventral mesodermal cores and ectoderm at 36 hpf (Fig. 3E,F). These results indicate that in wild type, *hand2* inhibits the transcription of intermediate-domain-Dlx genes from the ventral domain.

dlx3b/4b/5a has opposite regulatory effects to *hand2* on *gsc* and *nkx3.2* expression

The ventral inhibition of several Dlx genes by *hand2* suggests that *Dlx* and *hand2* may have some opposing roles in arch development. We examined the effect of *dlx3b/4b/5a* knockdown on two known *hand2* targets: *gsc* and *nkx3.2* (Miller et al., 2003), and the pre-skeletal marker *sox9a* [see Fig. S2 in the supplementary material, building upon Yan et al. (Yan et al., 2005)]. In the wild-type first arch, we see co-expression of the jaw-joint-region marker *nkx3.2* with *dlx4a* and *sox9a*, but not with *hand2* at 48 hpf (Fig. 4; see Fig. S3 in the supplementary material). *nkx3.2* expression is reduced in *dlx3b;4b;5a*-MO (Fig. 4J). Conversely, we see strong expansion of *nkx3.2* in *hand2*^{S6} mutants (Fig. 4K). The expanded *nkx3.2*-expressing cells in *hand2*^{S6} also express *sox9a* (Fig. 4C). When we inject *dlx3b;4b;5a*-MO into *hand2*^{S6} (*hand2*^{S6}*;dlx3b;4b;5a*-MO), *nkx3.2* expression is dramatically reduced (Fig. 4L), suggesting that *hand2* represses *nkx3.2* expression via its repression of *dlx3b/4b/5a*.

gsc is expressed in ventral and dorsal bands within the first two pharyngeal arches, avoiding the first arch intermediate domain (Fig. 4; see Fig. S3 in the supplementary material). In agreement with previous reports (Miller et al., 2003), ventral first arch *gsc* expression is lost in *hand2*^{S6} (Fig. 4O). Conversely, in *dlx3b;4b;5a*-MO there are low penetrance fusions of the dorsal and ventral *gsc* expression bands (Fig. 4N). In *hand2*^{S6}*;dlx3b;4b;5a*-MO, there is an overall reduction in *gsc* expression (Fig. 4P). However, in *hand2*^{S6}*;dlx3b;4b;5a*-MO there are sometimes small protrusions of *gsc* expression attached to the dorsal *gsc* domain (Fig. 4P). This ectopic *gsc* expression may represent expansions of the dorsal *gsc* domain. Hence, the wild-type function of *hand2* activates *gsc* and represses *nkx3.2* (in agreement with Miller et al., 2003), whereas *dlx3b/4b/5a* acts to repress *gsc* and activate *nkx3.2*.

The combined loss of *hand2* and *dlx3b/4b/5a* results in expansion of dorsal identity

The expansion of dorsal identity in *Dlx5*$^{-/-}$*;Dlx6*$^{-/-}$ mice (Depew et al., 2002) raises the issue of whether dorsal identity also expands in zebrafish injected with *dlx3b;4b;5a*-MO. To assay dorsal identity we used the dorsal muscle marker *eng2* (Hatta et al., 1990), which specifically labels a region of the first arch mesodermal core,

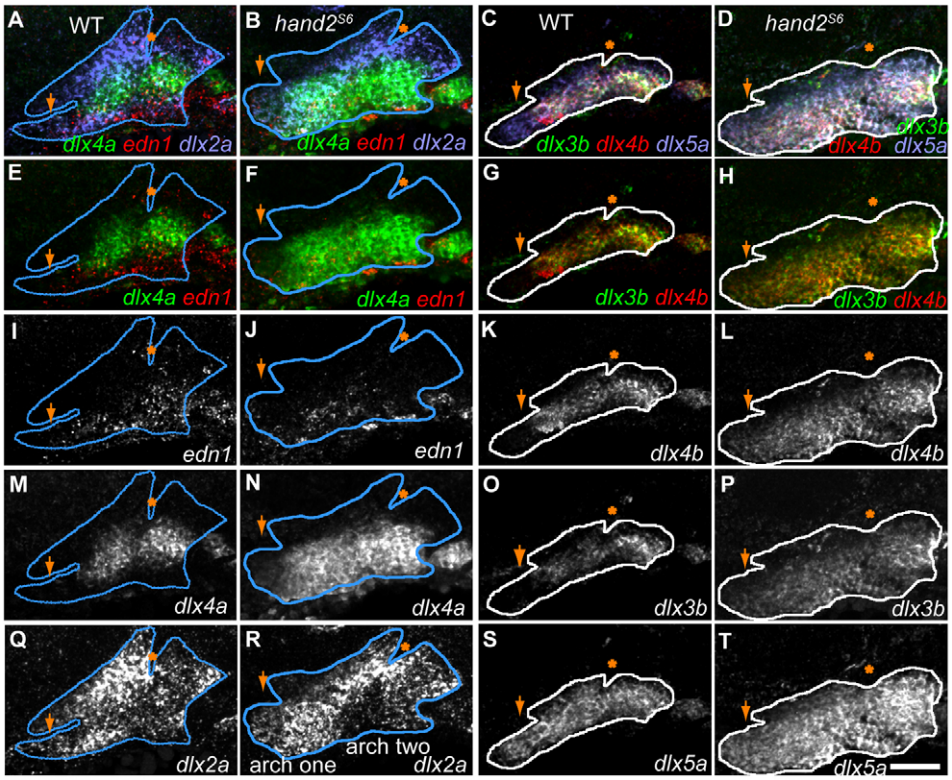

Fig. 3. *Dlx* expression expands ventrally in *hand2* mutants. Images are projections from confocal stacks of 36 hpf RNA in situ, with anterior leftwards, dorsal upwards. For context, *dlx2a* (blue lines) or *dlx5a* expression (white lines) is outlined in the first two arches. (**A**) In wild-type fish, *dlx4b* is expressed dorsal to the *edn1*-expressing mesoderm and ectoderm. However, in *hand2*^{S6} fish (**B**), *dlx4a* is expressed both within the ventral *edn1* expressing region and in the intermediate mesenchyme. Although expanded, *dlx4a* expression remains ventral to the. Similarly, compared with wild type (**C**), *dlx3b* and *dlx4b* expression expands into ventral regions of *hand2*^{S6} (**D**), while remaining ventral to stomodeum and first pouch. (**E-T**) Separated confocal channels from A-D. Scale bar: 50 μm. Arrows indicate stomodeum; asterisks indicate the first pouch.

dorsal to *dlx4a* expression (Fig. 5A). Injection of *dlx3b;4b;5a*-MO into wild-type fish causes an increase in *eng2* expression volume (Fig. 5N,U). However, these expanded *eng2* expression domains are still located dorsal to *dlx4a* expression (Fig. 5F). In *hand2*^{S6} mutants, *eng2* expression is found ventral to its location in wild type (Fig. 5O), supporting Miller et al. (Miller et al., 2003). In *hand2*^{S6}, ectopic ventral nodules of *eng2* expression sometimes appear within mesoderm ensconced by *dlx4a* expression (Fig. 5G). Although *hand2*^{S6} mutants show changes in *eng2* expression shape, the average volume of *eng2* expression in *hand2*^{S6} mutants does not differ from wild type (Fig. 5U). When *dlx3b;4b;5a*-MO is injected into *hand2*^{S6}, *eng2* expression expands in volume (Fig. 5U) and is ventrally elongated (Fig. 5H), indicating that *dlx3b/4b/5a* and *hand2* separately repress *eng2*. The overall expression of *dlx4a* is reduced in *hand2*^{S6}*;dlx3b;4b;5a*-MO (Fig. 5U), indicating a further loss of intermediate identity in these fish. Despite the shifting patterning domains seen with *dlx3b/4b/5a* and *hand2* loss, we see no change in overall arch size, as assayed by *dlx2a* expression (Fig. 5U). Collectively, these results indicate that *hand2* and *dlx3b/4b/5a* act in concert to inhibit dorsal identity in ventral/intermediate pharyngeal arches at 36 hpf.

Early arch expression domains map onto the developing skeleton

To clarify the connection between *hand2/Dlx* expression and skeletal domains, we co-labeled fish for *hand2* and Dlx gene expression alongside the pre-skeletal marker *sox9a*. Early in arch development, pharyngeal *sox9a*-expressing cells express *dlx2a* (see Figs S2, S3 in the supplementary material). However, by 60 hpf, most of the *Dlx* expression that we observe is lateral to *sox9a* expression (see Movie 1 in the supplementary material). *dlx2a* expression is maintained in cartilages near the Meckel's-palatoquadrate joint and the hyosymplectic-ceratohyal joint (Fig. 6A-C; see Fig. S2 in the supplementary material) and in mesenchyme lateral to these cartilages (see Movie 1 in the supplementary material). All arch expression of *dlx2a* is ventral to the neurocranium (see Fig. S2 in the supplementary material), consistent with previous findings (Verreijdt et al., 2006). *dlx5a* is expressed within cartilages in the Meckel's-palatoquadrate and the hyosymplectic-ceratohyal joint regions at 60 hpf. *dlx5a* is also expressed in mesenchyme lateral to much of the skeleton, except for dorsal aspects of the palatoquadrate cartilage, hyomandibular cartilage and most of the ceratohyal cartilage (Fig. 6E-L). *dlx5a*^{J1073aEt} expression is very similar to *dlx5a* in situ, but probably owing to the longevity of GFP proteins, *dlx5a*^{J1073aEt} is detectable in cartilages longer than *dlx5a* RNA (see Fig. S1 in the supplementary material). *dlx6a* expression is very similar to *dlx5a*, although the dorsal *dlx6a* expression border may not extend as far dorsally as *dlx5a* (Fig. 6I-L). Dlx3b and *dlx5a*^{J1073aEt} expression is found within precursor cells for both the opercle and branchiostegal bones (see Fig. S1 in the supplementary material). At 60 hpf, *dlx4a* expression is found in the Meckel's-palatoquadrate joint, and in the hyosymplectic-ceratohyal joint, as well as in mesenchymal cells lateral to these cartilages (Fig. 6M-P; see Movie 2 in the supplementary material). At 60 hpf, *dlx3b*, *dlx4b* and *dlx4a* show similar expression; however, as at 36 hpf, *dlx3b* is also strongly expressed in ectoderm (Fig. 6M-T and data not shown). By contrast, at 60 hpf, *hand2* is expressed within much of the Meckel's and ceratohyal cartilages, as well as the surrounding mesenchyme, ventral to *dlx3b* and *dlx4a* expression (Fig. 6M-T). Hence, the relative dorsoventral expression borders of *hand2* and the various Dlx genes are maintained from 36 hpf to 60 hpf, although outside of joint regions there is a progressive loss of Dlx gene expression in chondral elements. The D-I-V boundaries revealed by *hand2* and *Dlx* at 60 hpf reveal which skeletal elements are formed from each expression domain.

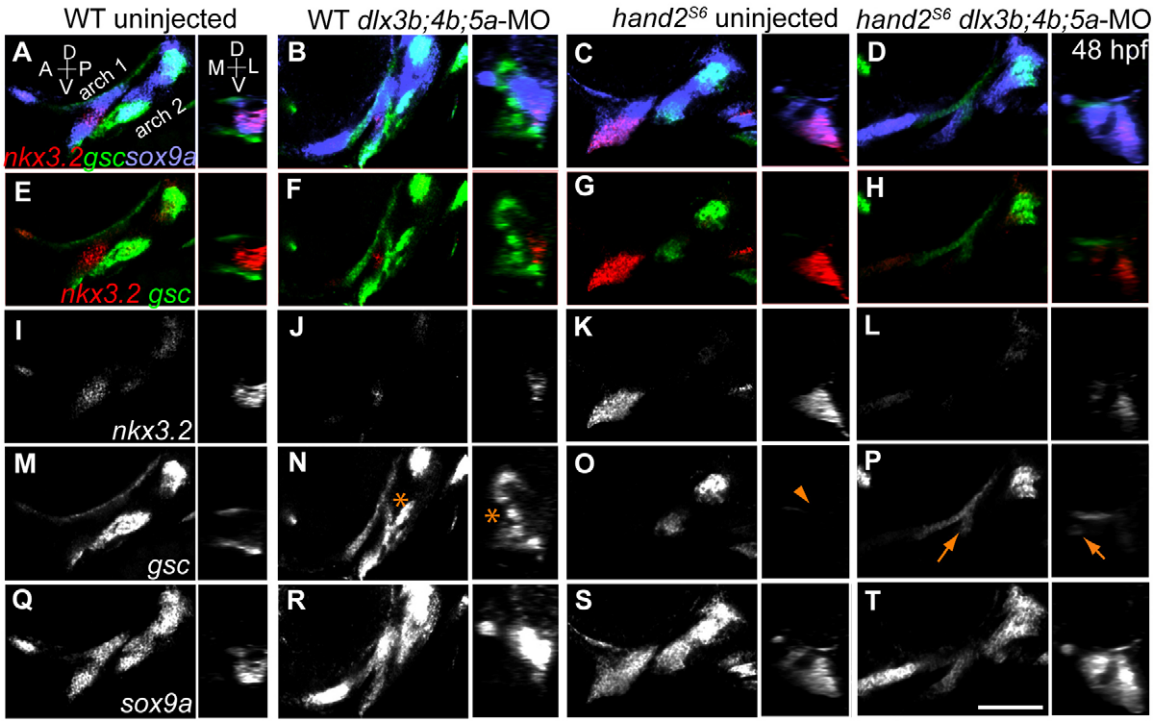

Fig. 4. *hand2* and *dlx3b/4b/5a* have opposing roles in regulating *gsc* and *nkx3.2*. (**A-T**) Lateral views (left; anterior leftwards, dorsal upwards) taken from single confocal sections of RNA in situs and reconstructed orthogonal sections (right; medial leftwards, dorsal upwards) through the first arch joint region of 48 hpf fish. Markers are indicated on the left panel of each row, and treatments are indicated above each column. *nkx3.2* expression is often reduced by (J) *dlx3b;4b;5a*-MO injection (80% penetrance), expanded in (K) uninjected *hand2*^{S6}, but reduced in (L) *hand2*^{S6}*;dlx3b;4b;5a*-MO. (N) In wild-type fish injected with *dlx3b;4b;5a*-MO, the dorsal and ventral *gsc* domains are occasionally (7% penetrance) found fused together (asterisk), medial to (F) *nkx3.2* expression. (O) In uninjected *hand2*^{S6} fish, ventral first arch *gsc* is lost, but some dorsal expression remains (arrowhead). (P) In *hand2*^{S6}*;dlx3b;4b;5a*-MO, ventral *gsc* is defective in arch one, and sometimes reduced (45% penetrance) in arch two, whereas ectopic *gsc* is seen attached to dorsal arch one expression (55% penetrance, arrow), medial to *nkx3.2*. Scale bar: 100 μm.

Skeletal elements are homeotically transformed with lowered function of *hand2* and *dlx3b/4b/5a*

Our expression data suggest that ventral arch cells lose their ventral identities and acquire intermediate identities in *hand2*-null mutants. When we also lower *dlx3b/4b/5a* functions, we see a gene expression shift, suggesting that dorsal identity expands. By these interpretations, we might also expect to see dorsalized homeotic phenotypes in arch-derived skeletons of such mutant and morpholino-injected fish. We constructed a phenotypic series of skeletal preparations to learn if the predicted homeosis is present (Fig. 7). Although there is extensive phenotypic variation (see Fig. S4 in the supplementary material), we found that the first arch skeletal phenotypes show the predicted changes most clearly.

In wild-type fish, there is a clear distinction between Meckel's and palatoquadrate shapes (Fig. 1A; Fig. 7A). In *dlx3b;4b;5a*-MO-injected fish, the jaw joint region is fused, but Meckel's cartilage is still immediately recognizable (Fig. 1D; see Fig. S4C in the supplementary material). Conversely, with just a partial loss of *hand2*, Meckel's cartilage is shortened, and the dentary bone is misshapen, but the joint-cleft between Meckel's and palatoquadrate cartilage is still clearly present (Fig. 7B; homozygous mutants for the *hand2* hypomorphic allele *c99*). However, with stronger loss of *hand2* function, the distinction between Meckel's and palatoquadrate is blurred (Fig. 7D, homozygotes for the *hand2* deficiency *s6*; and Fig. 7C, transheterozygotes of *S6* and *C99*). Instead, we interpret the midline cartilages in *hand2*^{S6} as being transformed into ectopic palatoquadrate cartilage. Consistent with this interpretation, structures shaped like ectopic pterygoid cartilages variably seen in the *hand2*^{S6} midline (arrows in Fig. 7C,D; Fig. S4E,F in the supplementary material). The ectopic expression of *dlx3b*, *dlx4b* and *dlx5a* seen in *hand2*^{S6} raises the possibility that the ectopic cartilages seen in *hand2*^{S6} require *dlx3b/4b/5a* function. Consistent with this hypothesis, the ectopic midline cartilages seen in *hand2*^{S6} homozygotes are reduced when *dlx3b;4b;5a*-MO is injected (Fig. 7E; Fig. 8D; Fig. S4D in the supplementary material). Instead, the cartilages protruding from the reduced palatoquadrate are shaped like ectopic pterygoid processes (arrows in Fig. 7E). Injection of *dlx5a*-MO, or co-injection of *dlx3b*-MO with *dlx4b*-MO into *hand2*^{S6} homozygotes produced subtler shifts in skeletal shape than injection of *dlx3b;4b;5a*-MO (see Fig. S4L in the supplementary material). When the hypomorphic *hand2*^{C99} homozygotes are injected with *dlx3b;4b;5a*-MO, these pterygoid shapes are also seen, and there is a remarkable symmetry along the dorsoventral axis, consistent with the predicted homeosis (arrows in Fig. 7F).

Joints are key structures in the intermediate domain, and thus are predicted to expand in *hand2* mutants. We used a transgenic line, *trps1*^{J1271aGt} (see Fig. 8P for details of the construct), in combination with cartilage labeling, to examine the joint and skeletal phenotypes more closely. *trps1*^{J1271aGt} is strongly expressed in joint regions of wild-type fish (Fig. 8A; matching our in situ results, not shown), consistent with findings in mouse (Kunath et al., 2002). Although reduced in intensity, we surprisingly see distinctive expression of *trps1*^{J1271aGt} in the joint region of *dlx3b;4b;5a*-MO-injected fish, even though a joint-cleft is lost (Fig.

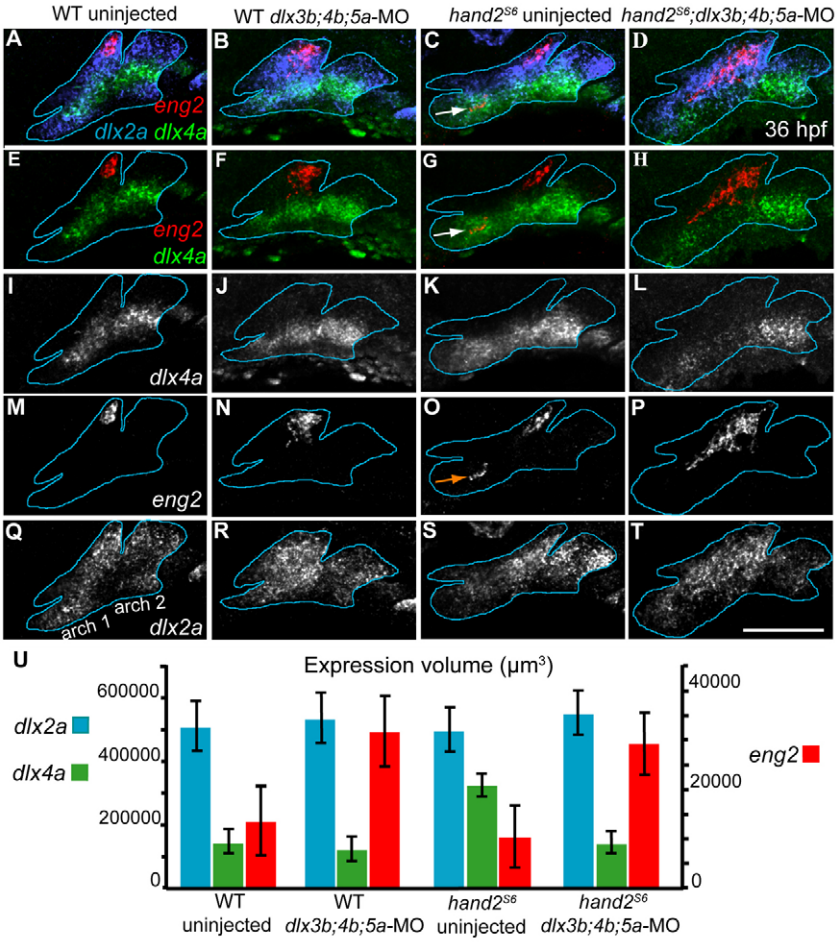

Fig. 5. *hand2* and *dlx3b/4b/5a* repress dorsal identity. (**A-T**) Projections of confocal stacks of 36 hpf RNA in situs. Arch one and two are outlined in blue, using *dlx2a* expression as a guide. Markers are indicated on the left panel of each row, and treatments indicated above each column. Anterior is leftwards, dorsal upwards. (O) In *hand2*^{S6}, ectopic *eng2* is indicated with an arrow. (**U**) Volumes (*y*-axis) of *dlx2a*, *dlx4a* and *eng2* expression. Error bars are 95% confidence intervals, from ANOVA. Measurements were made on confocal stacks of randomly selected fish, using the 'find objects by intensity' function in Volocity software. Intensity thresholds were adjusted from fish to fish, in order to accurately identify expression. There are no significant differences between fish classes in average intensity levels. Each bar shows the combined volumes of arches one to three, because these arches were sometimes identified as one object by the software. Scale bar: 100 µm.

8B). Instead, the *trps1*^{J127aAGt}-expressing cells lie just next to fused cartilages (Fig. 8B). In the corresponding region of *hand2*^{S6} fish, *trps1*^{j1271aGt} labeling was dramatically expanded (Fig. 8C), revealing expansion of joint-cell fate that is completely unrecognized by skeletal staining alone. In marked contrast, *trps1*^{j1271aGt} expression is highly reduced in the first arch of *hand2*^{S6}*;dlx3b;4b;5a*-MO compared with uninjected mutants, similar to *edn1* loss (Fig. 8D,E). Hence, we infer that joint cell identity is established by Edn1 signaling, is repressed by *hand2*, and requires *dlx3b/4b/5a* function.

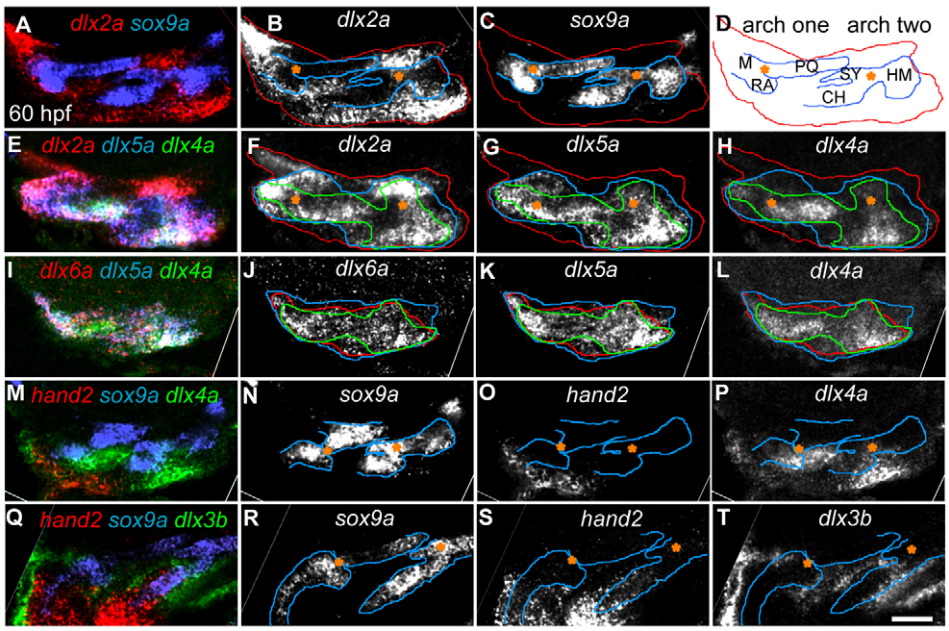

Fig. 6. The patterning domains delineated by Dlx genes and *hand2* can be connected to specific pre-skeletal shapes at 60 hpf. (**A-P**) Lateral views (anterior to the left, dorsal upwards) of RNA in situs confocal sections illustrate differences in dorsal expression boundaries, whereas ventral views (**Q-T**) (anterior towards the left, lateral upwards) illustrate ventral boundaries. (A-P) Merge of indicated markers is shown in the left column, whereas the other columns show single channels taken from the merge. Joints in the first two arches are indicated by asterisks. Confocal sections in I-L are lateral to cartilages, making the locations of underlying joints difficult to determine. Outlines in single channel panels follow the color schemes shown in the left column. CH, ceratohyal cartilage; HM, hyomandibular region; M, Meckel's cartilage ; PQ, palatoquadrate cartilage; RA, retroarticular process; SY, symplectic region. Scale bar: 50 µm.

DISCUSSION

The homeotic shape changes and molecular marker shifts we observe (Fig. 9B) indicate that *hand2* and Dlx genes impart distinct identities to D-I-V domains in the first two arches (Fig. 9C). In previous modeling, all Dlx genes were thought to be co-expressed with *hand2* in ventral aspects of arches (Depew and Simpson, 2006; Walker et al., 2006). Indeed, we show that there is initial co-expression of ventral *dlx4a* and *hand2*. However, *dlx3b*, *dlx4b* and *dlx4a* expression soon becomes restricted both dorsally and ventrally in the first two arches, indicating that by 36 hpf, zebrafish Dlx genes are more fully nested than was previously thought (Fig. 9). Intermediate-restricted Dlx nesting is also present in lamprey, which, together with our finding, suggests that dorsal/ventral Dlx restriction is basal within vertebrates (Daniel Medeiros, personal communication). We provide new evidence that *dlx3b*, *dlx4b* and *dlx5a* have overlapping functions in intermediate domain patterning, coincident with their overlapping expression within the intermediate domain. By 36 hpf, *hand2* is expressed ventral to *dlx4a*, correlating with its specific requirements in ventral domain patterning (Miller et al., 2003). The stacked expression of *dlx4a* and *hand2* persists until after major cartilage domains have been formed. We recognize that owing to the dynamic nature of gene expression, only precise fate maps can definitively connect expression patterns between different time-points. Nonetheless, the differential expression and requirements of *dlx1a/2a*, *hand2* and *dlx3b/4b/5a* provides a mechanism to generate discrete D-I-V domains within pharyngeal arches and skeleton (Fig. 9).

Similar to the findings in mouse (Qiu et al., 1997), zebrafish *dlx1a* and *dlx2a* function redundantly to pattern dorsal identity. However, more ventrally restricted Dlx genes *dlx3b/4b/5a* lack dorsal requirements, supporting a correlation between Dlx expression and function. We have also noted additional *Dlx* nesting: *dlx3b/4b* nest within the *dlx5a* expression domain. It will be important for future work to test the functional relevance of this deeper Dlx nesting, which may reveal patterning sub-domains.

Skeletal shape changes in Edn1 signaling pathway mutants are correlated with changes in *hand2* and *Dlx* expression. *mef2ca* and *furina* mutants, which only partially reduce Edn1 signaling, result in the loss of *dlx4b* and *dlx5a* expression, but no persistent losses in *hand2* expression (Miller et al., 2007; Walker et al., 2006). The skeletal defects in *mef2ca* and *furina* mutants include joint loss, ectopic cartilages and second arch bone fusion, but no ventral defects (Miller et al., 2007; Walker et al., 2006), similar to *dlx3b;4b;5a*-MO. By contrast, *edn1* mutants and *plcb3* mutants, in which Edn1 signaling is strongly reduced, have strong loss of *hand2*, *dlx3b* and *dlx5a* expression (Miller et al., 2000; Walker et al., 2006; Walker et al., 2007). The skeletal defects seen in *edn1* and *plcb3* mutants include severe defects in both intermediate and ventral skeleton (Miller et al., 2000; Walker et al., 2006; Walker et al., 2007), similar to *hand2*^{S6}*;dlx3b;4b;5*a-MO. Furthermore, prominent expansions of the dorsal marker *eng2* are seen in both *edn1* mutants (Miller et al., 2003) and *hand2*^{S6}*;dlx3b;4b;5a-MO*. Hence, the overall arch patterning domains identified in this study of *hand2/Dlx* expression and function closely mirror the domains identified previously from studies of Edn1 signaling.

We examined skeletal phenotypes in fish treated with morpholinos to various combinations of *dlx1a*, *dlx2a*, *dlx3b*, *dlx4b* and *dlx5a*, revealing redundant patterning roles for these genes. However, the conclusions we draw are limited because we lack known null alleles in any Dlx gene. Furthermore, all *dlx4a* and *dlx6a* morpholinos tested to date have failed to disrupt splicing convincingly, or produce any skeletal phenotype (data not shown). It will be very important for future studies to examine null alleles of Dlx genes. For example, zebrafish *dlx5a*$^{-}$*;dlx6a*$^{-}$ nulls could conclusively test whether loss of these

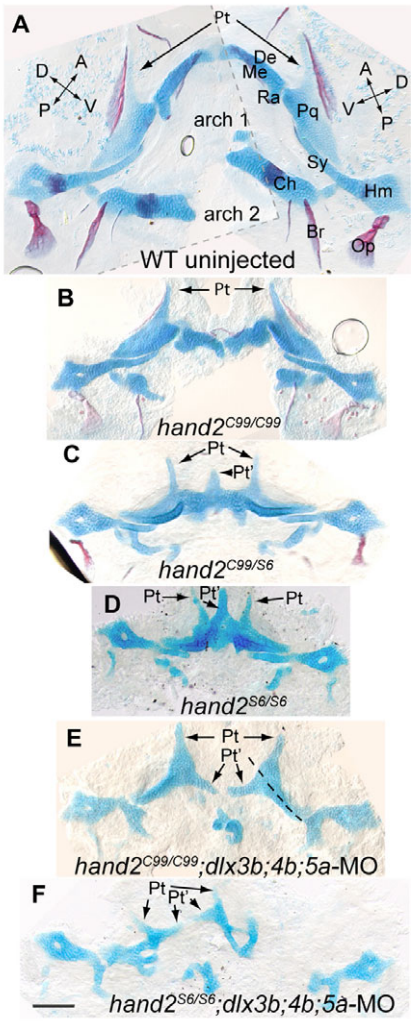

Fig. 7. *hand2* mutants and *hand2* mutants injected with *dlx3b;4b;5a*-MO show homeotic skeletal phenotypes. (A-F) Alcian Blue and Alizarin Red staining at 6 dpf. Images are flat mounted bilateral pharyngeal arches, oriented with midline to the center, and anterior upwards. (**A**) The wild-type skeleton was too large for a single image at this magnification, so two images were overlaid for this panel (border indicated with a broken grey line). (**B**) *hand2*^{C99} homozygotes have reduced ventral, but normal intermediate and dorsal domain skeleton. (**C**) In trans-heterozygous fish carrying *hand2*^{C99} and *hand2*^{S6}, defects are typically more severe than in *hand2*^{C99} homozygotes, but less severe than in (**D**) *hand2*^{S6} homozygotes. In *hand2*^{S6} homozygotes, broad cartilages often span the midline, similar in shape to duplicated palatoquadrates, complete with pterygoid processes (arrows). (**E**) When *hand2*^{C99} homozygotes are injected with *dlx3b;4b;5a*-MO, joints are lost in both arches, and the remainder of Meckel's cartilage is tapered out into a shape similar to a pterygoid process. A broken line indicates the first arch dorsal-ventral plane of symmetry. (**F**) The cartilage expansions of *hand2*^{S6} are lost when *dlx3b;4b;5a*-MO is injected. The palatoquadrate of *hand2*^{S6}*;dlx3b;4b;5a*-MO is often severely defective, though the distance between the first and second arch-derived skeleton seen on the left side of F is exaggerated by mounting artifacts. Scale bar: 100 μm.

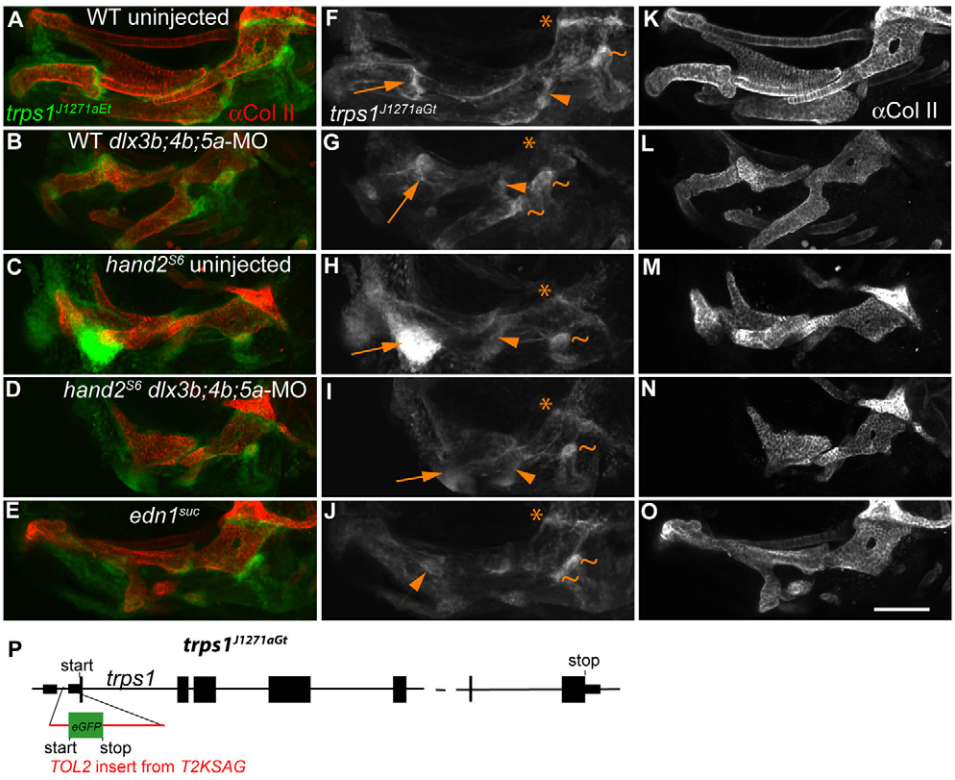

Fig. 8. Jaw joint expression of *trps1*^{J1271aGt} is regulated by Edn1 signaling, and the Edn1 targets *hand2* and *dlx3b/4b/5a*. (**A-O**) Confocal projections of 4 dpf anti-Collagen II and *trps1*^{J1271aGt} labeling is shown, merged in the left panel, and split in the center and right panels. Treatments are indicated in the left column. Anterior is leftwards, dorsal upwards. (A) In wild type, *trps1*^{J1271aGt} expression is faint in skeleton, and very bright in joints. (B) *dlx3b;4b;5a*-MO injection reduces *trps1*^{j1271aGt} in the first, (arrow) and second (arrowhead) arch joints, whereas the fused OP-BSR (tildes) bone expresses ectopic *trps1*^{j1271aGt}. (C) In *hand2*^{S6}, the jaw joint expression of *trps1*^{J1271aGt} expands dramatically, beneath broad ectopic cartilages. (D) In *hand2*^{S6}*;dlx3b;4b;5a*-MO, the expanded cartilages and *trps1*^{J1271aGt} expression domains in the first arch are reduced compared to uninjected *hand2*^{S6}. (E) In *edn1* mutants, the first and second arch joint expression of *trps1*^{J1271aGt} is lost, and conversely the opercle-hyomandibular joint expands. Throughout these treatments, the hyomandibular-neurocranium joint (asterisk) is normal. (**P**) Diagram of the J1271a insertion site in *trps1* (GenBank Accession Number, GU556967). Intronic sequence is not to scale. We identified the 5′ end (GenBank Accession Number, GU474515) of the *trps1* gene by 5′ RACE from a predicted, incomplete *trps1* sequence, ENSDART0000098144. *trps1* 5′ RACE revealed a single 5′ noncoding exon, with the J1271a integration site in the first intron. The splice acceptor orientation in T2KSAG predicts that it should be spliced into the processed message, with translation beginning at the initiating methionine in GFP, probably making J1271a a gene trap. Scale bar: 100 μm.

two genes in fish results in the homeotic transformations observed in *Dlx5*$^{-}$*;Dlx6*$^{-}$ mutant mice. Although we have demonstrated that *dlx3b/4a/4b* expression does not extend as far dorsally as *dlx5a/6a*, we have not observed a functional consequence of this expression difference. The expression difference between *dlx3b/4a/4b* and *dlx5a/6a* may be present because the major D-I-V domains are further subdivided into smaller patterning domains by *Dlx* expression. With genetic nulls, we could conclusively assay the functional relevance of expression differences between *dlx3b/4a/4b* and *dlx5a/6a*.

In wild-type zebrafish, *trps1* expression faithfully labels joint regions. However, in our mutants, we found several examples of *trps1*-expressing joint cells that do not connect skeletal elements. For example, although *dlx3b;4b;5a*-MO injection causes a fusion between Meckel's and palatoquadrate cartilages, some *trps1* expression is found in cells surrounding the location where the joint would have been. Similarly. some expression of *nkx3.2* remains, indicating that even when normally jointed cartilages are fused together, remnants of joint pattern can remain. In *dlx3b;4b;5a*-MO, *trps1* expression spans the fused opercle-branchiostegal bone, including a region of the bone that does not connect to skeleton. As a more extreme example, in *hand2*^{S6}, Meckel's cartilage is lost, and instead there is an enormous mass of ectopic *trps1*-expressing cells. In *hand2*^{S6}, the most anterior *trps1*-expressing cells sometimes extend well beyond any apparent bone or cartilage, indicating that joint cells can arise separately from skeleton. The disassociation of joint cells from jointed skeletons in our mutants leads us to ask how wild-type fish obtain a perfect correlation of jointed skeleton with jointing cells. It will be intriguing to discover the developmental relationship between joint cells and jointed skeletal elements.

Losses in ventral or intermediate domain identity result in compensatory expansion of identity from other domains (Fig. 9). When *hand2* is lost, *dlx3b*, *dlx4a*, *dlx4b* and *dlx5a* expression expands ventrally at 36 hpf. New research indicates that *hand2* also inhibits Dlx gene expression in mouse (David Clouthier, personal communication). Coincident with the expansion of these Dlx genes, we observe expansion of intermediate domain cartilages, *trps1* expression and *nkx3.2* expression in *hand2*^{S6}. Injecting *dlx3b;4b;5a*-MO into *hand2*^{S6} mutants results in a loss of joint identity, indicating that *hand2* represses joint identity via its repression *dlx3b/4b/5a*. When both *hand2* and *dlx3b/4b/5a* functions are reduced, the arch volume (indicated by 36 hpf *dlx2a* expression) remains fairly constant, and dorsal identity expands. The expansion of dorsal identity in *hand2*^{S6}*;dlx3b;4b;5a*-MO is similar to expansions of

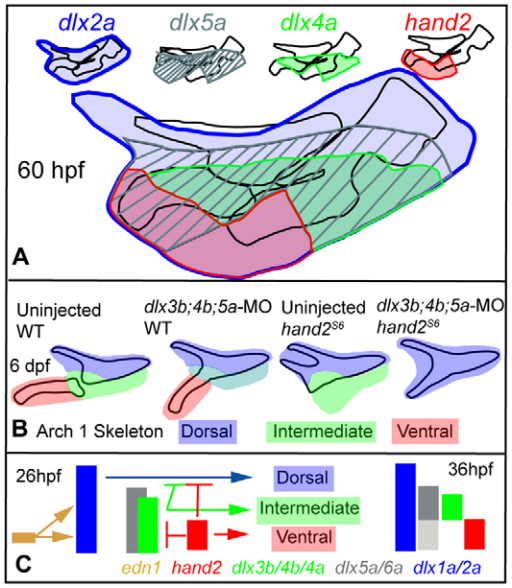

Fig. 9. A model of D-I-V pattern formation. (**A**) Schematic of gene expression domains relative to cartilaginous skeleton, based on our 60 hpf RNA in situ data. The relationships of bones to domains are described in the text. (**B**) Proposed homeotic shifts in dorsal, intermediate and ventral domains. In *dlx3b;4b;5a*-MO, intermediate identity is reduced, resulting in joint loss, whereas dorsal expands, causing a hybrid intermediate-dorsal identity (light blue). In *hand2* mutants, ventral identity is lost, whereas intermediate and dorsal identity expands. In *hand2* mutants injected with *dlx3b;4b;5a*-MO, both ventral and intermediate identity are lost, whereas dorsal identity expands. (**C**) A regulatory network for domain formation suggested by the patterning shifts observed in *edn1*, *hand2* and *dlx3b/4b/5a* knockdown. By 36 hpf, repression from *hand2* results in ventral loss of *dlx3b/4b/4a* in both arches, as well as second arch *dlx5a/6a* downregulation (light gray).

dorsal identity observed in Edn1 pathway mutants. For example, dorsalizing homeoses are seen in both zebrafish and mouse *Edn1* mutants (Kimmel et al., 2003; Ozeki et al., 2004), and *Ednra* mutants/morpholinos (Nair et al., 2007; Ruest et al., 2004), as well as mouse *Dlx5*$^{-}$*;Dlx6*$^{-}$ mutants (Beverdam et al., 2002; Depew et al., 2002). In our study, we examined markers broadly and specifically required for ventral and intermediate domain identity, but a broadly expressed dorsal domain specific marker has remained elusive. Candidates for dorsal specification genes have been recently proposed (Jeong et al., 2008; Zuniga et al., 2010).

Acknowledgements
We thank Macie Walker, Craig Miller, Ryan Macdonald, Gage Crump and April DeLaurier for comments during manuscript preparation. We thank Joseph Martial's lab for sharing a fluorescent in situ protocol prior to publication. We thank Jose Morillo and other members of the Johnson lab for identifying and maintaining enhancer or gene traps, and Ryan McAdow for identifying transposon insertion sites. We thank John Dowd and the UO fish facility for the care and maintenance of our fish. This work was supported by NIH grants DE13834, HD22486 (to C.B.K.), DK069466 (to S.L.J.) and DTG GM007257 (to J.C.T.). Deposited in PMC for release after 12 months.

Competing interests statement
The authors declare no competing financial interests.

Supplementary material
Supplementary material for this article is available at
http://dev.biologists.org/lookup/suppl/doi:10.1242/dev.049700/-/DC1

References

Akimenko, M. A., Ekker, M., Wegner, J., Lin, W. and Westerfield, M. (1994). Combinatorial expression of three zebrafish genes related to distal-less: part of a homeobox gene code for the head. *J. Neurosci.* **14**, 3475-3486.
Angelo, S., Lohr, J., Lee, K. H., Ticho, B. S., Breitbart, R. E., Hill, S., Yost, H. J. and Srivastava, D. (2000). Conservation of sequence and expression of Xenopus and zebrafish dHAND during cardiac, branchial arch and lateral mesoderm development. *Mech. Dev.* **95**, 231-237.
Beverdam, A., Merlo, G. R., Paleari, L., Mantero, S., Genova, F., Barbieri, O., Janvier, P. and Levi, G. (2002). Jaw transformation with gain of symmetry after Dlx5/Dlx6 inactivation: mirror of the past? *Genesis* **34**, 221-227.
Crump, J. G., Swartz, M. E. and Kimmel, C. B. (2004). An integrin-dependent role of pouch endoderm in hyoid cartilage development. *PLoS Biol.* **2**, E244.
Crump, J. G., Swartz, M. E., Eberhart, J. K. and Kimmel, C. B. (2006). Moz-dependent Hox expression controls segment-specific fate maps of skeletal precursors in the face. *Development* **133**, 2661-2669.
Depew, M. J. and Simpson, C. A. (2006). 21st century neontology and the comparative development of the vertebrate skull. *Dev. Dyn.* **235**, 1256-1291.
Depew, M. J., Lufkin, T. and Rubenstein, J. L. (2002). Specification of jaw subdivisions by Dlx genes. *Science* **298**, 381-385.
Depew, M. J., Simpson, C. A., Morasso, M. and Rubenstein, J. L. (2005). Reassessing the Dlx code: the genetic regulation of branchial arch skeletal pattern and development. *J. Anat.* **207**, 501-561.
Eberhart, J. K., Swartz, M. E., Crump, J. G. and Kimmel, C. B. (2006). Early Hedgehog signaling from neural to oral epithelium organizes anterior craniofacial development. *Development* **133**, 1069-1077.
Ekker, M., Wegner, J., Akimenko, M. A. and Westerfield, M. (1992). Coordinate embryonic expression of three zebrafish engrailed genes. *Development* **116**, 1001-1010.
Ellies, D. L., Stock, D. W., Hatch, G., Giroux, G., Weiss, K. M. and Ekker, M. (1997). Relationship between the genomic organization and the overlapping embryonic expression patterns of the zebrafish dlx genes. *Genomics* **45**, 580-590.
Ghanem, N., Jarinova, O., Amores, A., Long, Q., Hatch, G., Park, B. K., Rubenstein, J. L. and Ekker, M. (2003). Regulatory roles of conserved intergenic domains in vertebrate Dlx bigene clusters. *Genome Res.* **13**, 533-543.
Hatta, K., Schilling, T. F., BreMiller, R. A. and Kimmel, C. B. (1990). Specification of jaw muscle identity in zebrafish: correlation with engrailed-homeoprotein expression. *Science* **250**, 802-805.
Jeong, J., Li, X., McEvilly, R. J., Rosenfeld, M. G., Lufkin, T. and Rubenstein, J. L. (2008). Dlx genes pattern mammalian jaw primordium by regulating both lower jaw-specific and upper jaw-specific genetic programs. *Development* **135**, 2905-2916.
Jowett, T. and Yan, Y. L. (1996). Double fluorescent in situ hybridization to zebrafish embryos. *Trends Genet.* **12**, 387-389.
Kaji, T. and Artinger, K. B. (2004). dlx3b and dlx4b function in the development of Rohon-Beard sensory neurons and trigeminal placode in the zebrafish neurula. *Dev. Biol.* **276**, 523-540.
Kawakami, K., Takeda, H., Kawakami, N., Kobayashi, M., Matsuda, N. and Mishina, M. (2004). A transposon-mediated gene trap approach identifies developmentally regulated genes in zebrafish. *Dev. Cell* **7**, 133-144.
Kimmel, C. B., Ballard, W. W., Kimmel, S. R., Ullmann, B. and Schilling, T. F. (1995). Stages of embryonic development of the zebrafish. *Dev. Dyn.* **203**, 253-310.
Kimmel, C. B., Miller, C. T., Kruze, G., Ullmann, B., BreMiller, R. A., Larison, K. D. and Snyder, H. C. (1998). The shaping of pharyngeal cartilages during early development of the zebrafish. *Dev. Biol.* **203**, 245-263.
Kimmel, C. B., Ullmann, B., Walker, M., Miller, C. T. and Crump, J. G. (2003). Endothelin 1-mediated regulation of pharyngeal bone development in zebrafish. *Development* **130**, 1339-1351.
Kunath, M., Ludecke, H. J. and Vortkamp, A. (2002). Expression of Trps1 during mouse embryonic development. *Mech. Dev.* **1**, S117-S120.
Liu, D., Chu, H., Maves, L., Yan, Y. L., Morcos, P. A., Postlethwait, J. H. and Westerfield, M. (2003). Fgf3 and Fgf8 dependent and independent transcription factors are required for otic placode specification. *Development* **130**, 2213-2224.
Miller, C. T. and Kimmel, C. B. (2001). Morpholino phenocopies of endothelin 1 (sucker) and other anterior arch class mutations. *Genesis* **30**, 186-187.
Miller, C. T., Schilling, T. F., Lee, K., Parker, J. and Kimmel, C. B. (2000). sucker encodes a zebrafish Endothelin-1 required for ventral pharyngeal arch development. *Development* **127**, 3815-3828.
Miller, C. T., Yelon, D., Stainier, D. Y. and Kimmel, C. B. (2003). Two endothelin 1 effectors, hand2 and bapx1, pattern ventral pharyngeal cartilage and the jaw joint. *Development* **130**, 1353-1365.
Miller, C. T., Swartz, M. E., Khuu, P. A., Walker, M. B., Eberhart, J. K. and Kimmel, C. B. (2007). mef2ca is required in cranial neural crest to effect Endothelin1 signaling in zebrafish. *Dev. Biol.* **308**, 144-157.
Nair, S., Li, W., Cornell, R. and Schilling, T. F. (2007). Requirements for Endothelin type-A receptors and Endothelin-1 signaling in the facial ectoderm

for the patterning of skeletogenic neural crest cells in zebrafish. *Development* **134**, 335-345.
Nusslein-Volhard, C. (2002). *Zebrafish: a Practical Approach.* Oxford: Oxford University Press.
Ozeki, H., Kurihara, Y., Tonami, K., Watatani, S. and Kurihara, H. (2004). Endothelin-1 regulates the dorsoventral branchial arch patterning in mice. *Mech. Dev.* **121**, 387-395.
Panganiban, G. and Rubenstein, J. L. (2002). Developmental functions of the Distal-less/Dlx homeobox genes. *Development* **129**, 4371-4386.
Parinov, S., Sevugan, M., Ye, D., Yang, W. C., Kumaran, M. and Sundaresan, V. (1999). Analysis of flanking sequences from dissociation insertion lines: a database for reverse genetics in Arabidopsis. *Plant Cell* **11**, 2263-2270.
Park, B. K., Sperber, S. M., Choudhury, A., Ghanem, N., Hatch, G. T., Sharpe, P. T., Thomas, B. L. and Ekker, M. (2004). Intergenic enhancers with distinct activities regulate Dlx gene expression in the mesenchyme of the branchial arches. *Dev. Biol.* **268**, 532-545.
Qiu, M., Bulfone, A., Ghattas, I., Meneses, J. J., Christensen, L., Sharpe, P. T., Presley, R., Pedersen, R. A. and Rubenstein, J. L. (1997). Role of the Dlx homeobox genes in proximodistal patterning of the branchial arches: mutations of Dlx-1, Dlx-2, and Dlx-1 and -2 alter morphogenesis of proximal skeletal and soft tissue structures derived from the first and second arches. *Dev. Biol.* **185**, 165-184.
Ruest, L. B., Xiang, X., Lim, K. C., Levi, G. and Clouthier, D. E. (2004). Endothelin-A receptor-dependent and -independent signaling pathways in establishing mandibular identity. *Development* **131**, 4413-4423.
Sato, T., Kurihara, Y., Asai, R., Kawamura, Y., Tonami, K., Uchijima, Y., Heude, E., Ekker, M., Levi, G. and Kurihara, H. (2008). An endothelin-1 switch specifies maxillomandibular identity. *Proc. Natl. Acad. Sci. USA* **105**, 18806-18811.
Schulte-Merker, S., Hammerschmidt, M., Beuchle, D., Cho, K. W., De Robertis, E. M. and Nusslein-Volhard, C. (1994). Expression of zebrafish goosecoid and no tail gene products in wild-type and mutant no tail embryos. *Development* **120**, 843-852.
Sperber, S. M., Saxena, V., Hatch, G. and Ekker, M. (2008). Zebrafish dlx2a contributes to hindbrain neural crest survival, is necessary for differentiation of sensory ganglia and functions with dlx1a in maturation of the arch cartilage elements. *Dev. Biol.* **314**, 59-70.
Stock, D. W., Ellies, D. L., Zhao, Z., Ekker, M., Ruddle, F. H. and Weiss, K. M. (1996). The evolution of the vertebrate Dlx gene family. *Proc. Natl. Acad. Sci. USA* **93**, 10858-10863.
Stock, D. W., Jackman, W. R. and Trapani, J. (2006). Developmental genetic mechanisms of evolutionary tooth loss in cypriniform fishes. *Development* **133**, 3127-3137.
Sumiyama, K., Irvine, S. Q. and Ruddle, F. H. (2003). The role of gene duplication in the evolution and function of the vertebrate Dlx/distal-less bigene clusters. *J. Struct. Funct. Genomics* **3**, 151-159.
Verreijdt, L., Debiais-Thibaud, M., Borday-Birraux, V., Van der Heyden, C., Sire, J. Y. and Huysseune, A. (2006). Expression of the dlx gene family during formation of the cranial bones in the zebrafish (Danio rerio): differential involvement in the visceral skeleton and braincase. *Dev. Dyn.* **235**, 1371-1389.
Walker, M. B. and Kimmel, C. B. (2007). A two-color acid-free cartilage and bone stain for zebrafish larvae. *Biotech. Histochem.* **82**, 23-28.
Walker, M. B., Miller, C. T., Coffin Talbot, J., Stock, D. W. and Kimmel, C. B. (2006). Zebrafish furin mutants reveal intricacies in regulating Endothelin1 signaling in craniofacial patterning. *Dev. Biol.* **295**, 194-205.
Walker, M. B., Miller, C. T., Swartz, M. E., Eberhart, J. K. and Kimmel, C. B. (2007). phospholipase C, beta 3 is required for Endothelin1 regulation of pharyngeal arch patterning in zebrafish. *Dev. Biol.* **304**, 194-207.
Welten, M. C., de Haan, S. B., van den Boogert, N., Noordermeer, J. N., Lamers, G. E., Spaink, H. P., Meijer, A. H. and Verbeek, F. J. (2006). ZebraFISH: fluorescent in situ hybridization protocol and three-dimensional imaging of gene expression patterns. *Zebrafish* **3**, 465-476.
Westerfield, M. (1995). *The Zebrafish Book: A Guide for the Laboratory Use of Zebrafish (Danio Rerio).* Eugene, Oregon: University of Oregon Press.
Yan, Y. L., Miller, C. T., Nissen, R. M., Singer, A., Liu, D., Kirn, A., Draper, B., Willoughby, J., Morcos, P. A., Amsterdam, A. et al. (2002). A zebrafish sox9 gene required for cartilage morphogenesis. *Development* **129**, 5065-5079.
Yan, Y. L., Willoughby, J., Liu, D., Crump, J. G., Wilson, C., Miller, C. T., Singer, A., Kimmel, C., Westerfield, M. and Postlethwait, J. H. (2005). A pair of Sox: distinct and overlapping functions of zebrafish sox9 co-orthologs in craniofacial and pectoral fin development. *Development* **132**, 1069-1083.
Yanagisawa, H., Clouthier, D. E., Richardson, J. A., Charite, J. and Olson, E. N. (2003). Targeted deletion of a branchial arch-specific enhancer reveals a role of dHAND in craniofacial development. *Development* **130**, 1069-1078.
Yelon, D., Ticho, B., Halpern, M. E., Ruvinsky, I., Ho, R. K., Silver, L. M. and Stainier, D. Y. (2000). The bHLH transcription factor hand2 plays parallel roles in zebrafish heart and pectoral fin development. *Development* **127**, 2573-2582.
Zuniga, E., Stellabotte, F. and Crump, J. G. (2010). Jagged-Notch signaling ensures dorsal skeletal identity in the vertebrate face. *Development* **137**, 1843-1852.